Sparsity-Aware Joint Narrowband Interference and Impulse Noise Mitigation for Hybrid Powerline-Wireless Transmission

Mohamed Mokhtar*, Waheed U. Bajwa†, and Naofal Al-Dhahir*
*University of Texas at Dallas, USA, Emails: {m.mokhtar, aldhahir}@utdallas.edu
†Rutgers, The State University of New Jersey, Email: waheed.bajwa@rutgers.edu

***Abstract*—Exploiting multiple physical layers for communications has gained increasing interest recently to improve reliability and/or coverage range. Powerline and unlicensed wireless communication networks are attractive candidates to realize this objective because of their ubiquity. However, their performance can be severely degraded by impulsive noise (IN) and narrowband interference (NBI), respectively. In this paper, we exploit the inherent sparse structures of NBI and IN in the frequency and time domains, respectively, to propose an efficient joint estimation and mitigation scheme based on compressive sensing (CS) principles. Moreover, we investigate the metric of *maximum expected coherence* of our scheme for realistic powerline communication (PLC) and wireless channels, which provides some insight into its performance. Finally, our numerical experiments demonstrate the superiority of jointly processing the wireless and PLC channel outputs for CS-based NBI and IN mitigation over separate processing of individual channel outputs.**

I. Introduction

Receive diversity techniques are widely used in wireless systems to mitigate deleterious channel fading effects [1]. To further improve the reliability and/or increase the coverage range of broadband transmissions, there has been an increased interest in achieving additional diversity through multiple physical layers. Unlicensed wireless communication and powerline communication (PLC) have emerged as ideal candidates for this objective due to their ubiquity [2], [3].

In-home broadband PLC standards such as IEEE P1901.1 and ITU-T G.hn [4] use orthogonal frequency division multiplexing (OFDM) and operate in the 1.8–250 MHz frequency band. In-home broadband wireless local area networks (WLAN) standards such as IEEE 802.11g/n also use OFDM modulation and operate in the unlicensed 2.4 GHz and/or 5 GHz ISM frequency bands. In order to improve transmission reliability, a hybrid PLC-wireless system can simultaneously transmit OFDM symbols over both PLC and WLAN channels and can then jointly process the signals received by the PLC and WLAN modems for exploitation of the independence of the channel and interference characteristics of the two physical media. Note that while channel fading and interference in receive-diversity based wireless systems follow the same statistical distributions on all branches, these distributions are markedly different for the PLC and wireless branches.

Despite its advantages, a hybrid PLC-wireless system faces two main challenges. First, in-home PLC networks suffer from impulsive noise (IN) due to abrupt voltage changes caused by on-off switching of in-home appliances and power electronics devices such as silicon-controlled rectifiers, switching regulators, and brush motors [5]. Second, WLAN signals experience narrow-band interference (NBI) from co-existing wireless communication systems sharing the same frequency band such as cordless phones and Bluetooth devices [6]. Our goal in this paper is to investigate novel approaches for mitigation of this NBI and IN in hybrid PLC-wireless systems by exploiting the inherent sparse structures of NBI and IN in the frequency and time domains, respectively.

In terms of prior works, mitigation of NBI and IN in OFDM systems has been studied in [2], [3], [6], [7]. But [2], [3] do not exploit the sparse structures of NBI and IN. Also, [2] assumes flat-fading PLC and wireless channels, while [3] assumes them to be deterministic. Both [6] and [7] do exploit sparsity of NBI and IN to mitigate them using compressive sensing (CS) techniques [8]. They demonstrate that CS-based mitigation of NBI or IN performs much better than traditional interference cancelation schemes. However, both of these works focus on individual NBI and IN mitigation, as opposed to joint mitigation of NBI and IN in hybrid PLC-wireless systems.

To the best of our knowledge, this paper is the first to study joint mitigation of NBI and IN in hybrid PLC-wireless systems by jointly exploiting the sparsity of NBI and IN using CS techniques. To summarize, the main contributions of this paper are as follows. First, we develop a novel CS-based framework to jointly mitigate NBI and IN in hybrid PLC-wireless systems by exploiting their inherent sparsity in different domains. Our formulation in this regard accommodates multiple receive antennas and multiple PLC wires. Second, we heuristically motivate the gains associated with CS-based joint NBI and IN mitigation by investigating the metric of *maximum expected coherence* for realistic PLC and WLAN channel models. Finally, we quantify the gains of our approach through numerical experiments that compare the performances of joint and individual processing of PLC and WLAN received signals for a wide range of NBI and IN power levels.

Notation: Lower- and upper-case bold letters denote vectors and matrices, respectively. Also, $\mathbf{I}$ and $\mathbf{F}$ denote the identity and the Fast Fourier transform (FFT) matrices, respectively, while subscripts denote their sizes. The frequency domain matrices/vectors are denoted by $\mathbf{A}_x^{(i)}$/$\mathbf{a}_x^{(i)}$, where $x \in \{W, P\}$ denotes the transmission system with W and P for wireless and PLC systems, respectively, while the superscript i indicates the i^{th} antenna or wire. The corresponding time domain matrices/vectors are denoted by $\bar{\mathbf{A}}_x^{(i)}$/$\bar{\mathbf{a}}_x^{(i)}$. Finally, $(\cdot)^H$, $(\cdot)^*$, $(\cdot)^T$, $\mathbb{E}[\cdot]$, and $|\cdot|$ denote the complex-conjugate transpose, complex-conjugate, transpose, statistical expectation and absolute value operations, respectively.

Paper Organization: Our system model, assumptions for hybrid indoor PLC-wireless networks, and the problem for-

This work is supported by NPRP grant # NPRP 6-070-2-024 from the Qatar National Research Fund (a member of Qatar Foundation). The statements made herein are solely the responsibility of the authors.

mulation are described in Section II. Our CS-based approach for joint mitigation of NBI and IN, and our discussion of maximum expected coherence are presented in Section III. Finally, numerical experiments and concluding remarks are provided in Sections IV and V, respectively.

II. System Model

We consider single-input-multiple-output (SIMO) OFDM-based simultaneous transmissions over PLC and wireless systems [3] (see Fig. 1). The wireless system operates in an unlicensed WLAN band and consists of a single-antenna transmitter and a receiver equipped with K antennas. The PLC receiver can process up to $\beta \in \{1,2,3\}$ outputs over its 3 wires. We assume each antenna at the wireless receiver suffers from uncorrelated NBI and the 3 wires of the PLC channel experience uncorrelated IN.[1] Under these assumptions, the received signals at the k^{th}, $k \in \{1,\ldots,K\}$, antenna and the j^{th}, $j \in \{1,\ldots,\beta\}$, wire are respectively given by:

$$\bar{\mathbf{y}}_W^{(k)} = \bar{\mathbf{H}}_W^{(k)}\bar{\mathbf{x}} + \bar{\mathbf{i}}_W^{(k)} + \bar{\mathbf{n}}_W^{(k)}, \quad \text{and} \tag{1}$$

$$\bar{\mathbf{y}}_P^{(j)} = \bar{\mathbf{H}}_P^{(j)}\bar{\mathbf{x}} + \bar{\mathbf{i}}_P^{(j)} + \bar{\mathbf{n}}_P^{(j)}, \tag{2}$$

where the subscripts W and P denote the wireless and PLC systems, respectively. Here, assuming M OFDM subcarriers, $\bar{\mathbf{H}}_W^{(k)}$ and $\bar{\mathbf{H}}_P^{(j)}$ denote $M \times M$ circulant channel matrices between the transmitter's antenna/wire and the $k^{\text{th}}/j^{\text{th}}$ receiver's antenna/wire of the wireless and PLC systems, respectively. The first columns of these matrices are $\begin{bmatrix} \bar{\mathbf{h}}_W^{(k)T} & \mathbf{0}_{1\times M-L_W} \end{bmatrix}^T$ and $\begin{bmatrix} \bar{\mathbf{h}}_P^{(j)T} & \mathbf{0}_{1\times M-L_P} \end{bmatrix}^T$, where $\bar{\mathbf{h}}_W^{(k)}$ and $\bar{\mathbf{h}}_P^{(j)}$ are the wireless and PLC channel impulse response (CIR) vectors with L_W and L_P complex taps, respectively. We assume that the wireless CIR taps are Rayleigh distributed, while the PLC CIR taps are log-normal distributed [2]. In addition, we assume the availability of perfect channel state information (CSI) at the wireless and PLC receivers. Using $\mathbf{x}$ for the $M\times 1$ OFDM data symbols vector, $\bar{\mathbf{x}}$ in (1), (2) is defined as $\bar{\mathbf{x}} = \mathbf{F}_M^*\mathbf{x}$. Further, $\bar{\mathbf{n}}_W^{(k)}$ and $\bar{\mathbf{n}}_P^{(j)}$ denote complex zero-mean circularly-symmetric additive-white-Gaussian noise (AWGN) vectors at the $k^{\text{th}}/j^{\text{th}}$ receiver's antenna/wire with variances σ_W^2 and σ_P^2, respectively. Finally, the NBI (which is sparse in the frequency domain) and the IN (which is sparse in the time domain) effects at each antenna/PLC wire are denoted by $\bar{\mathbf{i}}_W^{(k)}$ and $\bar{\mathbf{i}}_P^{(j)}$, respectively.

Notice that we can take the FFT of (1) and (2) to obtain

$$\underbrace{\mathbf{F}_M\bar{\mathbf{y}}_W^{(k)}}_{\triangleq \mathbf{y}_W^{(k)}} = \underbrace{\mathbf{F}_M\bar{\mathbf{H}}_W^{(k)}\mathbf{F}_M^*}_{\triangleq \Lambda_W^{(k)}}\mathbf{x} + \underbrace{\mathbf{F}_M\bar{\mathbf{i}}_W^{(k)}}_{\triangleq \mathbf{i}_W^{(k)}} + \underbrace{\mathbf{F}_M\bar{\mathbf{n}}_W^{(k)}}_{\triangleq \mathbf{n}_W^{(k)}}, \text{ and} \tag{3}$$

$$\underbrace{\mathbf{F}_M\bar{\mathbf{y}}_P^{(j)}}_{\triangleq \mathbf{y}_P^{(j)}} = \underbrace{\mathbf{F}_M\bar{\mathbf{H}}_P^{(j)}\mathbf{F}_M^*}_{\triangleq \Lambda_P^{(j)}}\mathbf{x} + \mathbf{F}_M\bar{\mathbf{i}}_P^{(j)} + \underbrace{\mathbf{F}_M\bar{\mathbf{n}}_P^{(j)}}_{\triangleq \mathbf{n}_P^{(j)}}, \tag{4}$$

where $\Lambda_W^{(k)}$ and $\Lambda_P^{(j)}$ are $M \times M$ diagonal matrices whose diagonal elements (denoted by $\begin{bmatrix} h_{W,1}^{(k)} & \ldots & h_{W,M}^{(k)} \end{bmatrix}$ and $\begin{bmatrix} h_{P,1}^{(j)} & \ldots & h_{P,M}^{(j)} \end{bmatrix}$) are the channel frequency response (CFR) coefficients of the $k^{\text{th}}/j^{\text{th}}$ receiver's antenna/wire of the wireless channel/PLC output, respectively. Here, $\mathbf{i}_W^{(k)}$ denotes the frequency-domain (FD) NBI vector at the k^{th} antenna. In particular, the sparsity of NBI (in frequency) and IN (in time) means $\|\mathbf{i}_W^{(k)}\|_0 \triangleq \rho_W^{(k)} \ll M$ and $\|\bar{\mathbf{i}}_P^{(j)}\|_0 \triangleq \rho_P^{(j)} \ll M$, where $\|\cdot\|_0$ counts the number of nonzero entries of a vector.

Concatenating the received wireless and PLC signals in (3) and (4) for all $k \in \{1,\ldots,K\}$ and $j \in \{1,\ldots,\beta\}$ into a single column vector results in

$$\underbrace{\begin{bmatrix} \mathbf{y}_W^{(1)} \\ \vdots \\ \mathbf{y}_W^{(K)} \\ \mathbf{y}_P^{(1)} \\ \vdots \\ \mathbf{y}_P^{(\beta)} \end{bmatrix}}_{\triangleq \mathbf{y}} = \underbrace{\begin{bmatrix} \Lambda_W^{(1)} \\ \vdots \\ \Lambda_W^{(K)} \\ \Lambda_P^{(1)} \\ \vdots \\ \Lambda_P^{(\beta)} \end{bmatrix}}_{\triangleq \mathbf{G}} \mathbf{x} + \underbrace{\begin{bmatrix} \mathbf{i}_W^{(1)} \\ \vdots \\ \mathbf{i}_W^{(k)} \\ \mathbf{F}_M\bar{\mathbf{i}}_P^{(1)} \\ \vdots \\ \mathbf{F}_M\bar{\mathbf{i}}_P^{(\beta)} \end{bmatrix}}_{\triangleq \mathbf{i}} + \underbrace{\begin{bmatrix} \mathbf{n}_W^{(1)} \\ \vdots \\ \mathbf{n}_W^{(K)} \\ \mathbf{n}_P^{(1)} \\ \vdots \\ \mathbf{n}_P^{(\beta)} \end{bmatrix}}_{\triangleq \mathbf{n}}. \tag{5}$$

Here, we term the $M(K+\beta)\times 1$ vector $\mathbf{y}$ as the *measurement vector*, while we term the $M(K+\beta)\times M$ matrix $\mathbf{G}$ as the *measurement matrix*. Note that $\mathbf{G}$ comprises the CFR matrices of the wireless and PLC channels, $\mathbf{G} \triangleq \begin{bmatrix} \mathbf{G}_W^H & \mathbf{G}_P^H \end{bmatrix}^H$, where $\mathbf{G}_W$ and $\mathbf{G}_P$ denote the concatenated FD channel matrices for wireless and PLC channels, respectively. Finally, $\mathbf{i}$ denotes the combined $M(K+\beta)\times 1$ NBI and IN vectors, while $\mathbf{n}$ is the equivalent $M(K+\beta)\times 1$ FD noise vector. Our main goal here is to use (5) for estimation of the NBI and IN vectors.

III. CS-Based Joint Estimation of NBI and IN

In order to estimate NBI and IN from $\mathbf{y}$, we first get rid of the unknown term $\mathbf{G}\mathbf{x}$ in (5) by projecting $\mathbf{y}$ onto the left-null space of $\mathbf{G}$ using the following projection matrix [6], [7]: $\mathbf{Q} = \mathbf{I}_{M(K+\beta)} - \mathbf{G}\mathbf{G}^\dagger$, where $\mathbf{G}^\dagger$ denotes the Moore-Penrose pseudoinverse of $\mathbf{G}$ that is given by $\left(\mathbf{G}^H\mathbf{G}\right)^{-1}\mathbf{G}^H$ for the case of a full column rank $\mathbf{G}$. Since $\mathbf{Q}\mathbf{G} = \mathbf{0}_{M(K+\beta)\times M}$, we obtain the following expression after this projection step:

$$\mathbf{y}' \triangleq \mathbf{Q}\mathbf{y} = \mathbf{Q}\mathbf{i} + \mathbf{Q}\mathbf{n} \triangleq \mathbf{Q}_{\text{eqn}}\mathbf{i}_{\text{eqn}} + \mathbf{n}'. \tag{6}$$

Here, $\mathbf{i}_{\text{eqn}} \triangleq \begin{bmatrix} \mathbf{i}_W^{(1)^T} & \ldots & \mathbf{i}_W^{(K)^T} & \bar{\mathbf{i}}_P^{(1)^T} & \ldots & \bar{\mathbf{i}}_P^{(\beta)^T} \end{bmatrix}^T$, $\mathbf{n}' \triangleq \mathbf{Q}\mathbf{n}$, and the *modified measurement matrix* $\mathbf{Q}_{\text{eqn}}$ is defined in terms of $\mathbf{Q}$ as follows:

$$\mathbf{Q}_{\text{eqn}} = \mathbf{Q}\begin{bmatrix} \mathbf{I}_{KM} & \mathbf{0}_{KM\times\beta M} \\ \mathbf{0}_{\beta M\times KM} & \mathbf{I}_\beta \otimes \mathbf{F}_M \end{bmatrix}, \tag{7}$$

where $\otimes$ denotes the Kronecker product operation.

A few remarks are in order now for $\mathbf{Q}_{\text{eqn}}$. First, $\mathbf{Q}_{\text{eqn}}$ has a closed-form expression due to the special structure of $\mathbf{Q}$ and $\mathbf{G}$ which can be decomposed into diagonal matrices. In particular, it follows after some manipulations that

$$\mathbf{Q} = \mathbf{I}_{M(K+\beta)} - \begin{bmatrix} \mathbf{G}_W\mathbf{G}_W^H & \mathbf{G}_W\mathbf{G}_P^H \\ \mathbf{G}_P\mathbf{G}_W^H & \mathbf{G}_P\mathbf{G}_P^H \end{bmatrix} \times (\mathbf{I}_{K+\beta} \otimes \Psi) \tag{8}$$

[1] This is a worst-case assumption since spatial correlation between the outputs of the PLC and/or wireless system can be exploited to further mitigate IN and NBI effects; see, e.g., [9] for an example from DSL systems.

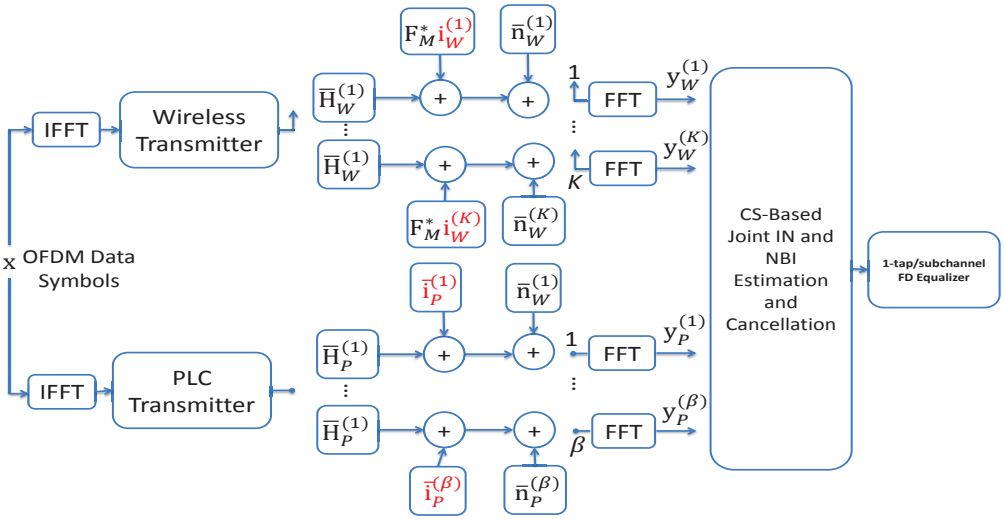

Fig. 1. A block diagram of the system model of a SIMO hybrid wirless/PLC system. Here, red fonts are used to indicate sparse vectors.

with the matrix Ψ being defined as follows:

$$\Psi \triangleq \left[\Lambda_W^{(1)}\left(\Lambda_W^{(1)}\right)^H + \ldots + \Lambda_W^{(K)}\left(\Lambda_W^{(K)}\right)^H + \Lambda_P^{(1)}\left(\Lambda_P^{(1)}\right)^H + \ldots + \Lambda_P^{(\beta)}\left(\Lambda_P^{(\beta)}\right)^H\right]^{-1}.$$

In particular, under the assumption of perfect CSI, $\mathbf{Q}$ can be efficiently computed since it mainly involves computing the inverse of diagonal matrix Ψ of size $M \times M$. Second, the columns of $\mathbf{Q}_{\text{eqn}}$ have same ℓ_2-norms in expectation. Due to space limitations, we only argue this fact heuristically. Since we intend to keep the average received power fixed, we can assume without loss of generality that the average wireless and PLC channel powers, given by $\mathbb{E}\left[\left|\bar{\mathbf{h}}_W^{(k)H}\bar{\mathbf{h}}_W^{(k)}\right|^2\right]$ and $\mathbb{E}\left[\left|\bar{\mathbf{h}}_P^{(j)H}\bar{\mathbf{h}}_P^{(j)}\right|^2\right]$, $\forall k,j \in \{1,\ldots,K\}$ and $\{1,\ldots,\beta\}$, respectively, are normalized to one. Next, since the CIR taps are assumed independent, the CFR coefficients have equal variances [10]. Using these facts, our statement can be established after some manipulations.

We have now reduced our problem of NBI and IN estimation to the linear model (6). While one can attempt to use traditional estimation approaches in this setting to estimate $\mathbf{i}_{\text{eqn}}$, we know from [6]–[8] that exploitation of the sparsity of $\mathbf{i}_{\text{eqn}}$ can result in much better performance. Specifically, the CS theory suggests to estimate sparse vectors by solving problems of the form (6) as follows:

$$\hat{\mathbf{i}}_{\text{eqn}} \triangleq \underset{\mathbf{i}\in\mathbb{C}^{(K+\beta)M}}{\text{argmin}} \|\mathbf{Q}_{\text{eqn}}\mathbf{i} - \mathbf{y}'\|_2^2 \quad \text{subject to} \quad \|\mathbf{i}\|_0 = S, \quad (9)$$

where S is the number of nonzero elements of $\mathbf{i}_{\text{eqn}}$, defined as $S \triangleq \sum_{k=1}^{K}\rho_W^{(k)} + \sum_{j=1}^{\beta}\rho_P^{(j)}$.

Note that while (9) in its stated form has combinatorial complexity, there exist a number of greedy and optimization-based approaches in the CS literature that can be used to solve this problem in an efficient manner. In this paper, we promote the use of a well-known greedy algorithm, termed *orthogonal matching pursuit* (OMP) [11], which estimates $\hat{\mathbf{i}}_{\text{eqn}}$ by iteratively selecting S columns of $\mathbf{Q}_{\text{eqn}}$ that are most correlated with the observations $\mathbf{y}'$ and then solving a *restricted* least-squares problem using the selected columns. We have chosen OMP for its computational simplicity and we summarize its main steps in the following.

Inputs: Vector $\mathbf{y}'$, matrix $\mathbf{Q}_{\text{eqn}}$, and sparsity level S.

Initialization: Define index set $I_0 = \{\}$, and set residual $\mathbf{r}_0 = \mathbf{y}'$, estimate $\hat{\mathbf{i}}_{\text{eqn}} = \mathbf{0}_{(K+\beta)M}$, and iteration count $l = 1$.

The l^{th} iteration:

1) Compute $\delta_i = \left|\mathbf{r}_{l-1}^H\mathbf{Q}_{\text{eqn}}(:,i)\right|$ for all $i \notin I_{l-1}$.
2) Choose index of the next nonzero entry computed during the l^{th} iteration as $c_l = \underset{i}{\text{argmax}}\ \delta_i$.
3) Update the indices of nonzero entries as $I_l = I_{l-1} \cup c_l$.
4) Set $\hat{\mathbf{i}}_{\text{eqn}}(I_l) = \left(\mathbf{Q}_{\text{eqn}}(:,I_l)\right)^{\dagger}\mathbf{y}$, where $\hat{\mathbf{i}}_{\text{eqn}}(I_l)$ denotes the elements of $\hat{\mathbf{i}}_{\text{eqn}}$ that are indexed by I_l.
5) Compute the residual error term at the l^{th} iteration as $\mathbf{r}_l = \mathbf{y} - \mathbf{Q}_{\text{eqn}}(:,I_l)\mathbf{i}_{\text{eqn}}(I_l)$.
6) If $l = S$ then exit, else set $l = l+1$ and go to Step 1.

We conclude our discussion of CS-based joint estimation of NBI and IN by noting that our scheme can be improved by imposing individual sparsity constraints on the NBI and IN components of $\mathbf{i}_{\text{eqn}}$ in (9). Also, it can be further improved by getting rid of the worst-case assumption that the PLC and wireless outputs are uncorrelated. This assumption means that the supports of NBI and IN in $\mathbf{i}_{\text{eqn}}$ are generally non-overlapping. But we expect spatial correlations in practical systems, which would lead to overlapping NBI and IN supports in $\mathbf{i}_{\text{eqn}}$ and which can be exploited for improved performance. We will pursue these improvements in future works.

A. Preliminary Analysis

While we carry out extensive numerical experiments in Section IV to demonstrate the superiority of our proposed scheme, we are also interested in an analytical understanding of its performance. It is now well understood in the CS literature [8] that the performance of any sparse recovery method is a function of some measure/property of the measurement matrix ($\mathbf{Q}_{\text{eqn}}$ in our case) [12]. In particular, the performance of OMP tends to be inversely proportional to the correlations between the (normalized) columns of $\mathbf{Q}_{\text{eqn}}$ [12], [13]. While

an exact specification of these correlations is beyond the scope of this paper, we carry out an analysis of these correlations in expectation to develop some insights into the performance of our proposed scheme. Specifically, we analyze the *maximum expected coherence* of $\mathbf{Q}_{\text{eqn}}$ in the following, which we define as follows:[2] $\bar{\mu}_{\max} \triangleq \max_{i,j:i\neq j} \{\mathbb{E}\left[\left|\mathbf{Q}_{\text{eqn}}(:,i)^H \mathbf{Q}_{\text{eqn}}(:,j)\right|\right]\}$. It is important to note here that $\bar{\mu}_{\max}$ is just an expected measure of correlations between the columns of $\mathbf{Q}_{\text{eqn}}$ and, as such, a small $\bar{\mu}_{\max}$ cannot guarantee that OMP will necessarily perform well for our setup. Nonetheless, a large $\bar{\mu}_{\max}$ (close to 1) will suggest that the modified measurement matrix under consideration is not well suited for sparse recovery problems.

To characterize $\bar{\mu}_{\max}$ for our problem, we proceed as follows. Using the definition of $\mathbf{Q}_{\text{eqn}}$ in (7) and the fact that $\mathbf{Q}$ is a projection matrix (i.e., $\mathbf{Q}^H\mathbf{Q} = \mathbf{Q}\mathbf{Q} = \mathbf{Q}$), we obtain

$$\mathbf{Q}_{\text{eqn}}(:,i)^H \mathbf{Q}_{\text{eqn}}(:,j) = \tag{10}$$
$$\mathbf{e}_i^H \begin{bmatrix} \mathbf{I}_{KM} & \mathbf{0}_{KM\times\beta M} \\ \mathbf{0}_{\beta M\times KM} & \mathbf{I}_\beta \otimes \mathbf{F}_M^H \end{bmatrix} \mathbf{Q} \begin{bmatrix} \mathbf{I}_{KM} & \mathbf{0}_{KM\times\beta M} \\ \mathbf{0}_{\beta M\times KM} & \mathbf{I}_\beta \otimes \mathbf{F}_M \end{bmatrix} \mathbf{e}_j,$$

where $\mathbf{e}_i$ is an $M \times 1$ unit vector whose i^{th} entry is equal to one and whose other entries are equal to zero. Next, we substitute the expression for $\mathbf{Q}$ derived in (8) into (10) to obtain $\mathbf{Q}_{\text{eqn}}(:,i)^H \mathbf{Q}_{\text{eqn}}(:,j)$ as shown in (11) on the top of the next page. We can see in (11) that the expression for $|\mathbf{Q}_{\text{eqn}}(:,i)^H \mathbf{Q}_{\text{eqn}}(:,j)|, i \neq j$, involves a 2×2 block matrix. The (1,1) block of it consists of diagonal matrices, with the (q,u) diagonal submatrix, $q,u = 1,\ldots,K$, having entries

$$\left|\left[\Lambda_W^{(q)} \left(\Lambda_W^{(u)}\right)^H \Psi\right]_{v,v}\right| = \tag{12}$$
$$\frac{\left|h_{W,v}^{(q)}\right| \left|h_{W,v}^{(u)}\right|}{\left|h_{W,v}^{(1)}\right|^2 + \ldots + \left|h_{W,v}^{(K)}\right|^2 + \left|h_{P,v}^{(1)}\right|^2 + \ldots + \left|h_{P,v}^{(\beta)}\right|^2},$$

where $[.]_{v,z}$ denotes the (v,z) entry of a given matrix. Moreover, blocks (1,2) and (2,1) are conjugate transposes of each other, with the (v,z) entry of the (q,u) submatrix, $q = 1,\ldots,K, u = 1,\ldots,\beta$, in the (1,2) block given by

$$\left|\left[\Lambda_W^{(q)} \left(\Lambda_P^{(u)}\right)^H \Psi \mathbf{F}_M\right]_{v,z}\right| = \tag{13}$$
$$\frac{\frac{1}{\sqrt{M}} \left|h_{W,v}^{(q)}\right| \left|h_{P,v}^{(u)}\right|}{\left|h_{W,v}^{(1)}\right|^2 + \ldots + \left|h_{W,v}^{(K)}\right|^2 + \left|h_{P,v}^{(1)}\right|^2 + \ldots + \left|h_{P,v}^{(\beta)}\right|^2}.$$

Finally, block (2,2) comprises circulant matrices, which are completely defined by their first rows. In particular, the first row of its (q,u) submatrix, $q,u = 1,\ldots,\beta$, is $\frac{1}{\sqrt{M}} \left(\text{diag}\left[\Lambda_P^{(q)} \left(\Lambda_P^{(u)}\right)^H \Psi\right]\right)^T \mathbf{F}_M^*$.

Notice from this discussion that the denominator in each entry of the block matrices in (11) decreases with an increase in the number of received outputs. This in turn implies that the quantity $|\mathbf{Q}_{\text{eqn}}(:,i)^H \mathbf{Q}_{\text{eqn}}(:,j)|, i \neq j$, reduces. Consequently, the maximum expected coherence $\bar{\mu}_{\max}$ reduces as well. This analytical observation can also be heuristically justified by noting that an increase in the number of outputs increases the dimension of the column space of the modified measurement matrix. It then reduces the possibility that any two columns of the modified measurement matrix will be highly correlated. We conclude from this that $\bar{\mu}_{\max}$ is a function of the PLC and wireless CFRs. In the next section, we will numerically evaluate $\bar{\mu}_{\max}$ for practical PLC and wireless channel characteristics as well as for different values of K and β. We will be normalizing the columns of $\mathbf{Q}_{\text{eqn}}$ in those experiments and evaluating the closeness of $\bar{\mu}_{\max}$ to 1 in that setting.

[2]We are forgoing normalization of the columns of $\mathbf{Q}_{\text{eqn}}$ here to simplify the evaluation of $\bar{\mu}_{\max}$, which is justified by virtue of the fact that the columns of $\mathbf{Q}_{\text{eqn}}$ have same norms on average.

IV. Numerical Results

In this section, we report the results of our numerical experiments to evaluate the performance of our proposed CS-based scheme for joint mitigation of NBI and IN in hybrid PLC-wireless systems. Our experimental setup corresponds to $K = 3, \beta = 3$ and $M = 64$, and our comparison is with a setup involving CS-based separate wireless and PLC processing. In terms of wireless modeling, we assume wireless channels with a uniform power delay profile, $L_W = 8$ zero-mean complex Gaussian taps, and normalized powers: $\mathbb{E}\left[|\bar{\mathbf{h}}_W^{(k)H} \bar{\mathbf{h}}_W^{(k)}|^2\right] = 1,\ k \in \{1,2,3\}$. We also assume the receive antennas suffer from independent contiguous narrowband interferers that occupy independent subcarrier indices and whose amplitudes are independent zero-mean complex Gaussian taps with fixed NBI-to-background Gaussian noise (NBI-GN) ratio, defined as $\frac{\mathbb{E}\left[\mathbf{i}_W^{(k)H} \mathbf{i}_W^{(k)}\right]}{\sigma_W^2},\ \forall\ k \in \{1,2,3\}$. Finally, we assume each narrowband interferer has a fixed width of 3 contiguous subcarriers, i.e., $\rho_W^{(k)} = 3,\ \forall\ k \in \{1,2,3\}$. This setup is similar to a Bluetooth signal (with 1 MHz bandwidth) interfering with an IEEE 802.11 g/n signal (with 20 MHz bandwidth) [14], and is of high practical interest due to commonly collocated Bluetooth and WLAN signals in the 2.4 GHz frequency band.

In terms of PLC modeling, we assume each PLC channel consists of two equal-power taps, i.e., $L_p = 2$, having uniformly-distributed phases and lognormal distributed magnitudes with standard deviations of 0.6 [2], [15]. We once again work with unit-power channels, $\mathbb{E}\left[|\bar{\mathbf{h}}_P^{(j)H} \bar{\mathbf{h}}_P^{(j)}|^2\right] = 1,\ \forall\ j \in \{1,2,3\}$, while we assume the IN is spread over 3 contiguous time samples, i.e., $\rho_P^{(j)} = 3,\ \forall\ j \in \{1,2,3\}$. Finally, we assume a fixed IN-to-background Gaussian noise (IN-GN) ratio, defined as $\frac{\mathbb{E}\left[\bar{\mathbf{i}}_P^{(j)H} \bar{\mathbf{i}}_P^{(j)}\right]}{\sigma_P^2},\ j \in \{1,2,3\}$.

To quantify the performance of our proposed scheme in terms of NBI and IN estimation accuracy, we use the performance metric of *average error vector magnitude* (AEVM), which we define as $\eta \triangleq \frac{\sum_{u=1}^{U} \|\mathbf{i}_{\text{eqn}} - \hat{\mathbf{i}}_{\text{eqn}}\|_2^2}{\sum_{u=1}^{U} \|\mathbf{i}_{\text{eqn}}\|_2^2}$ with U denoting the number of channel realizations ($U = 5000$ in these experiments). Note that a smaller value of η indicates better estimation performance. In Fig. 2, we plot η for both joint (our scheme) and separate processing for different NBI-GN and IN-GN levels. Two conclusions can be drawn from this figure. First, the higher the NBI-GN and IN-GN levels, the better the estimation performance for both joint and separate

$$\mathbf{Q}_{\text{eqn}}(:,i)^H\mathbf{Q}_{\text{eqn}}(:,j) = \mathbf{e}_i^H\mathbf{I}_{M(K+\beta)}\mathbf{e}_j \tag{11}$$

$$-\mathbf{e}_i^H\left[\begin{array}{ccc|ccc} \Lambda_W^{(1)}\left(\Lambda_W^{(1)}\right)^H\Psi & \dots & \Lambda_W^{(1)}\left(\Lambda_W^{(K)}\right)^H\Psi & \Lambda_W^{(1)}\left(\Lambda_P^{(1)}\right)^H\Psi\mathbf{F}_M & \dots & \Lambda_W^{(1)}\left(\Lambda_P^{(\beta)}\right)^H\Psi\mathbf{F}_M \\ \vdots & & \vdots & \vdots & & \vdots \\ \Lambda_W^{(K)}\left(\Lambda_W^{(1)}\right)^H\Psi & \dots & \Lambda_W^{(K)}\left(\Lambda_W^{(K)}\right)^H\Psi & \Lambda_W^{(K)}\left(\Lambda_P^{(1)}\right)^H\Psi\mathbf{F}_M & \dots & \Lambda_W^{(K)}\left(\Lambda_P^{(\beta)}\right)^H\Psi\mathbf{F}_M \\ \hline \mathbf{F}_M^H\Psi\Lambda_P^{(1)}\left(\Lambda_W^{(1)}\right)^H & \dots & \mathbf{F}_M^H\Psi\Lambda_P^{(1)}\left(\Lambda_W^{(K)}\right)^H & \mathbf{F}_M^H\Lambda_P^{(1)}\left(\Lambda_P^{(1)}\right)^H\Psi\mathbf{F}_M & \dots & \mathbf{F}_M^H\Lambda_P^{(1)}\left(\Lambda_P^{(\beta)}\right)^H\Psi\mathbf{F}_M \\ \vdots & & \vdots & \vdots & & \vdots \\ \mathbf{F}_M^H\Psi\Lambda_P^{(\beta)}\left(\Lambda_W^{(1)}\right)^H & \dots & \mathbf{F}_M^H\Psi\Lambda_P^{(\beta)}\left(\Lambda_W^{(K)}\right)^H & \mathbf{F}_M^H\Lambda_P^{(\beta)}\left(\Lambda_P^{(1)}\right)^H\Psi\mathbf{F}_M & \dots & \mathbf{F}_M^H\Lambda_P^{(\beta)}\left(\Lambda_P^{(\beta)}\right)^H\Psi\mathbf{F}_M \end{array}\right]\mathbf{e}_j$$

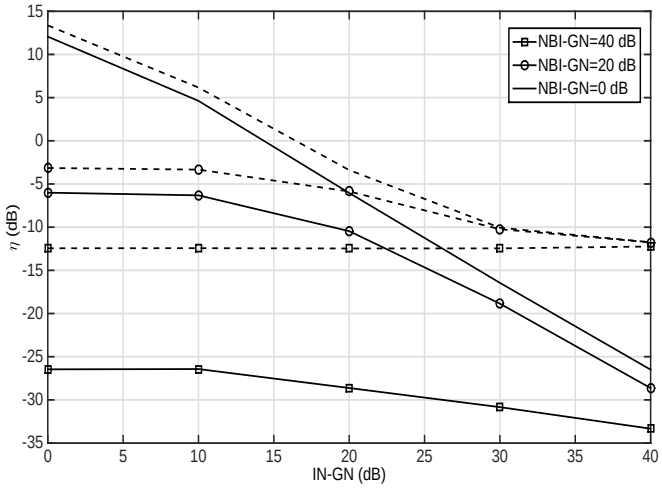

Fig. 2. AEVM for joint (solid lines) and separate (dashed lines) processing for different NBI-GN and IN-GN levels.

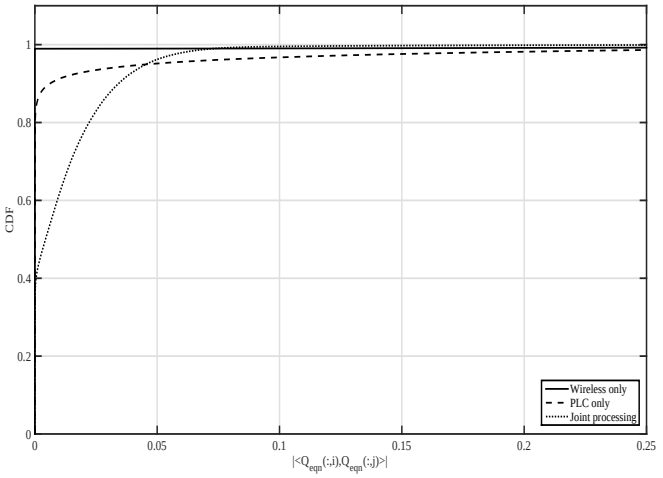

Fig. 3. CDF for the inner products of the modified measurement matrix columns.

processing. Second, and most importantly, our joint processing always leads to better performance than separate processing.

Fig. 3 shows the empirical cumulative distribution function (CDF) of the inner products of all the (normalized) measurement matrix columns in case of joint and separate processing. The total numbers of the inner product terms for joint, wireless and PLC outputs are equal to $(M(K+\beta))^2 - M(K+\beta)$, $(MK)^2 - MK$, and $(M\beta)^2 - M\beta$, respectively. This figure shows that the inner product magnitudes are sufficiently less than 1, which points to the likely success of OMP for joint sparse recovery of the IN and NBI signals [12], [13].

Next, we discussed in Section III that the metric of $\bar{\mu}_{\max}$ can be used to roughly understand if the modified measurement matrix (which is a function of the PLC and wireless channel characteristics) would result in reliable estimation. We evaluate $\bar{\mu}_{\max}$ in Table I, which shows that joint processing results in a smaller $\bar{\mu}_{\max}$. Note that for wireless-only processing, $\bar{\mu}_{\max} = 1$ for $K = 2$ because of the special structure of the modified measurement matrix in that case, which results in some of the columns being fully-correlated. But this can be avoided by either resorting to joint processing or using a carefully-designed precoder matrix such that the equivalent measurement matrix has smaller $\bar{\mu}_{\max}$. (For example, one could use a unitary random precoder matrix with independent and identically-distributed zero-mean Gaussian elements, as in [6].) Note that fully-correlated columns do not arise during PLC-only processing since the FFT matrix essentially acts as a precoder in the (2,2) block of $\mathbf{Q}_{\text{eqn}}$ in (7). Finally, separate processing always leads to a full-rank measurement matrix with no left null space in the case of a single antenna or wire. In this case, pilot subcarriers can be exploited as in [6], [7] to make the measurement matrix rank deficient and, hence, have a non-trivial left null space.

TABLE I
MAXIMUM EXPECTED COHERENCE FOR DIFFERENT ANTENNAS AND WIRES CONFIGURATIONS

	Joint processing	Wireless only	PLC only
$K=3,\ \beta=3$	0.19	0.47	0.28
$K=3,\ \beta=2$	0.24	0.47	0.55
$K=2,\ \beta=3$	0.24	1	0.28
$K=2,\ \beta=2$	0.32	1	0.55

Next, we present bit-error rate (BER) results in Fig. 4. Our results are plotted as a function of the signal-to-background-noise ratio (SNR) for fixed signal-to-NBI (S-NBI) and signal-to-IN ratios, defined as $\frac{\mathbb{E}\left[\mathbf{x}^H\mathbf{x}\right]}{\mathbb{E}\left[\mathbf{i}_W^{(k)H}\mathbf{i}_W^{(k)}\right]}$ and $\frac{\mathbb{E}\left[\mathbf{x}^H\mathbf{x}\right]}{\mathbb{E}\left[\mathbf{i}_P^{(j)H}\mathbf{i}_P^{(j)}\right]}$ $\forall\ k,j \in \{1,2,3\}$, respectively. In this paper, we assume for simplicity the same SNR for both the PLC and wireless systems, although these could be different in practice. Finally, our results are for the spectral efficiency of $R = 4$ bits/sec/Hz.

We compare four setups in Fig. 4 to quantify the performance gain of joint processing. In the first setup, NBI and IN are treated as noise and maximal ratio combining (MRC) is used to combine the received wireless and PLC signals.

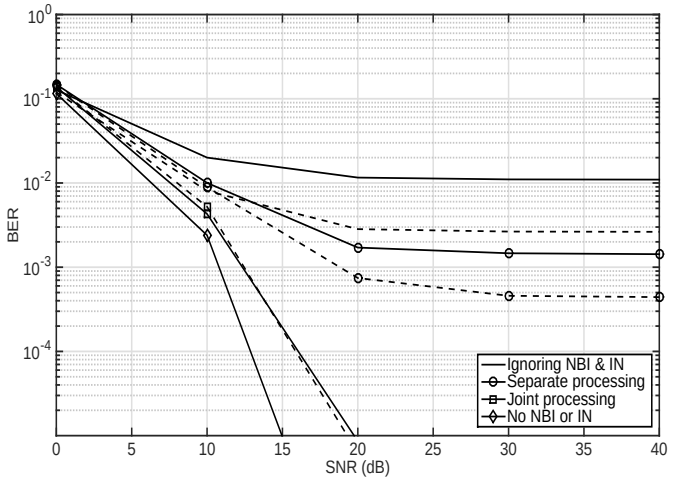

Fig. 4. BER performance for $R = 4$ bits/sec/Hz with solid and dashed lines for S-NBI and S-IN ratios equal to -10 dB and -5 dB, respectively

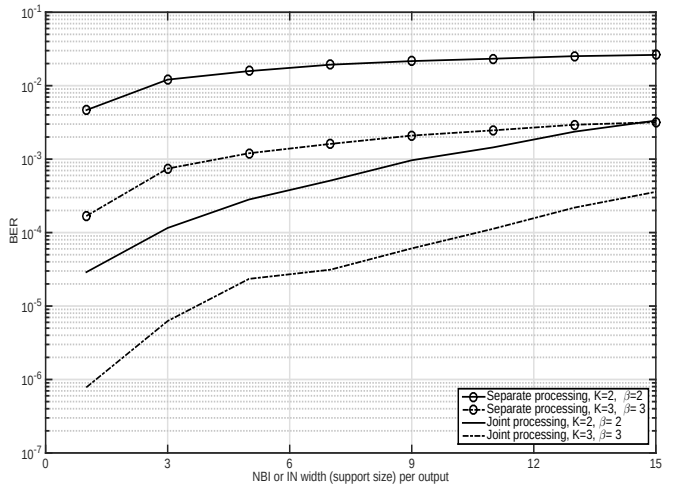

Fig. 5. BER performance for S-NBI and S-IN equal to -5 dB while SNR=20 dB, respectively, with $R = 4$ bits/sec/Hz

The second setup corresponds to separate processing in which each system individually estimates and cancels NBI or IN, and then MRC is used to combine both signals. Since it is shown in [6], [7] that CS-based techniques outperform conventional approaches to NBI and IN suppression, this setup corresponds to CS-based individual NBI and IN estimation. The figure shows that the NBI/IN cannot be completely canceled in this setup and the residual NBI/IN results in an error floor. The third setup represents the case of NBI and IN cancellation using our proposed approach, which is able to eliminate the error floor of [6], [7]. In particular, our proposed method is able to approach the performance of the fourth setup that corresponds to NBI and IN-free output.

We further quantify the performance gains of joint processing over separate processing in Fig. 5. This figure plots the BER as a function of the NBI and IN widths (support sizes) per output, which we assume to be the same at each antenna and wire, respectively. Since increasing the NBI and/or IN widths reduces sparsity, it results in a higher BER. However, joint processing is still able to significantly outperform separate processing in this decreased sparsity setting.

V. Conclusion and Future Work

We developed a new framework to jointly estimate and cancel NBI and IN in hybrid PLC-wireless systems by exploiting the sparsity of NBI and IN in the frequency and time domains, respectively. In addition, we analyzed the metric of maximum expected coherence of our scheme and showed that this metric does not approach one in the case of joint processing. Furthermore, we carried out extensive numerical experiments to demonstrate the superiority of our proposed joint PLC-wireless processing scheme over separate processing schemes.

While our initial results are encouraging, a number of aspects of this problem remain to be addressed. These aspects, which will be the focus of our future work, include:

- In this paper, we considered synchronous NBI interferers that lie exactly on the receiver FFT bins. In practice, the received signal can experience asynchronous NBI with fixed frequency offsets, which results in NBI power leakage across the FFT bins and destroys the sparsity of the NBI. To overcome this problem, we can apply receiver windowing (e.g., Hamming and Hanning windows) to reduce the NBI energy leakage and restore its sparse structure in the frequency domain as done in [6].
- While we assumed the practical case of the NBI and IN bins/samples being contiguous, we did not exploit this property to achieve further performance gains. CS theory provides us with powerful tools to recover signals that exhibit block-sparse structures with non-zero entries concentrated in clusters (see, e.g., [16]). Therefore, it is of great interest to investigate the performance gains and complexity trade-offs of these algorithms and compare them with the simple OMP algorithm used in this paper.

References

[1] J. G. Proakis, *Digital Communication*, 4th ed. McGraw-Hill, 2001.

[2] S. Guzelgoz, H. Celebi, and H. Arslan, "Analysis of a MultiChannel Receiver: Wireless and PLC Reception," in *Proc. EUSIPCO*, Aug. 2010.

[3] S. Lai and G. Messier, "Using the Wireless and PLC Channels for Diversity," *IEEE Trans. Commun.*, pp. 3865–3875, Dec 2012.

[4] V. Oksman and J. Zhang, "G.HNEM: The New ITU-T Standard on Narrowband PLC Technology," *IEEE Comm. Mag.*, Dec. 2011.

[5] H. Ferreira, L. Lampe, J. Newbury, and T. Swart, *Power Line Communications: Theory and Applications for Narrowband and Broadband Communications over Power Lines*. John Wiley & Sons, 2010.

[6] A. Gomaa and N. Al-Dhahir, "A Sparsity-Aware Approach for NBI Estimation in MIMO-OFDM," *IEEE Trans. Wireless Comm.*, Jun. 2011.

[7] G. Caire, T. Al-Naffouri, and A. Narayanan, "Impulse Noise Cancellation in OFDM: An Application of Compressed Sensing," in *Proc. IEEE Intl. Symp. Information Theory (ISIT)*, Jul. 2008, pp. 1293–1297.

[8] E. Candes, J. Romberg, and T. Tao, "Stable Signal Recovery from Incomplete and Inaccurate Measurements," *Comm. Pure App. Math.*, vol. 59, no. 9, pp. 1207–1223, Mar 2006.

[9] A. Awasthi, N. Al-Dhahir, O. Eliezer, and P. Balsara, "Alien Crosstalk Mitigation in Vectored DSL Systems for Backhaul Applications," in *Proc. IEEE Intl. Conf. Commun. (ICC)*, Jun. 2012, pp. 3852–3856.

[10] S. Krone and G. Fettweis, "Capacity Analysis for OFDM Systems with Transceiver I/Q Imbalance," in *Proc. IEEE GLOBECOM*, Nov. 2008.

[11] Y. Pati, R. Rezaiifar, and P. Krishnaprasad, "Orthogonal Matching Pursuit: Recursive Function Approximation with Applications to Wavelet Decomposition," in *Proc. Asilomar Conf. Sig., Syst. and Comp.*, 1993.

[12] W. Bajwa and A. Pezeshki, "Finite Frames for Sparse Signal Processing," in *Finite Frames*. Birkhuser Boston, 2012, ch. 10, pp. 303–335.

[13] J. Tropp, "Greed is Good: Algorithmic Results for Sparse Approximation," *IEEE Trans. Inf. Th.*, vol. 50, no. 10, pp. 2231–2242, Oct. 2004.

[14] E. Perahia and R. Stacey, *Next Generation Wireless LANs*. Cambridge University Press, 2013.

[15] S. Galli, "A Novel Approach to the Statistical Modeling of Wireline Channels," *IEEE Trans. Commun.*, pp. 1332–1345, May 2011.

[16] Y. Eldar, P. Kuppinger, and H. Bolcskei, "Block-Sparse Signals: Uncertainty Relations and Efficient Recovery," *IEEE Transactions on Signal Processing,*, vol. 58, no. 6, pp. 3042–3054, Jun. 2010.